Photoelectrochemical Etching Technology for Gallium Nitride Crystals

SCIOCS Co., Ltd.
Business Development Department
Fumimasa Horikiri
Noboru Fukuhara
Masatomo Shibata

Gallium nitride (GaN) has been intensively studied for applications in various optical and electronic devices. In terms of the device fabrication process, etching technology is one of the most important factors affecting device performance. Generally, GaN is etched by inductively coupled plasma reactive ion etching, because it has excellent chemical stability. However, plasma can easily damage GaN surfaces. This report presents photoelectrochemical etching technology with simple set-up for damage-free GaN etching.

Introduction

Gallium nitride (GaN) is widely used for opto applications, e.g., laser diodes and light-emitting diodes.[1] GaN electronic devices are becoming popular for mobile base stations to reduce energy consumption and meet 4G-5G application demands.[2] In addition, GaN power devices have recently attracted considerable research attention as energy-saving solutions because of their low specific on-resistance coupled with a high breakdown voltage.[3] These advantages arise from the high electron-drift velocity and high breakdown field of GaN compared with those of Si and GaAs.[4]

In terms of the device fabrication process, etching is one of the most important factors affecting device performance, namely stability, reliability and in-plane uniformity of device operation. For GaN-based devices, plasma-assisted dry etching, such as inductively coupled plasma reactive ion etching, has commonly been used because wet chemical etching is fairly difficult due to the very strong chemical bonding between nitrogen and group-III atoms.[5] However, there is a serious problem by using dry etching, that is, high-energy ions induce etching damage to the surface, such as nitrogen-vacancy defects and disordered atomic-bond arrangements. Thus, it leads to degraded performance of the device.

PEC etching technology for GaN

Photoelectrochemical (PEC) etching is one of the wet etching technologies. Photo-assisted anodic oxidation is the basis of PEC etching of GaN. GaN dissolves into Ga^{3+} ions due to the excitation of holes by the ultraviolet (UV) irradiation at the anode of the GaN/electrolyte interface, where electrons flow into the outside circuit. The Ga^{3+} ions react with hydroxide ions (OH^-) in the electrolyte, resulting in the formation of Ga_2O_3, which dissolves in an acid or base. Thus, an anodic oxidation process is the basis of PEC etching of GaN. PEC etching was first reported by M. S. Minsky et al. in 1996 as a GaN wet-etching technology.[6] Many reports on GaN PEC etching are available.[7)–11)] The conventional PEC etching process is shown schematically in **Fig. 1**.[12] Conventional PEC etching requires sealing the electrolyte between the GaN surface anode and the cathode, and UV irradiation over the GaN bandgap energy ($\lambda < 365$ nm), then an anodic oxidation process of GaN surface occurs.

$$GaN(s) + 3h^+ \rightarrow Ga^{3+} + 1/2N_2(g)\uparrow \quad (1)$$

$$Ga^{3+} + 3OH^- \rightarrow 1/2Ga_2O_3 + 3/2H_2O(l) \quad (2)$$

The hydrogen evolution reaction occurs at the cathode, where electrons flow in from the outside circuit, as

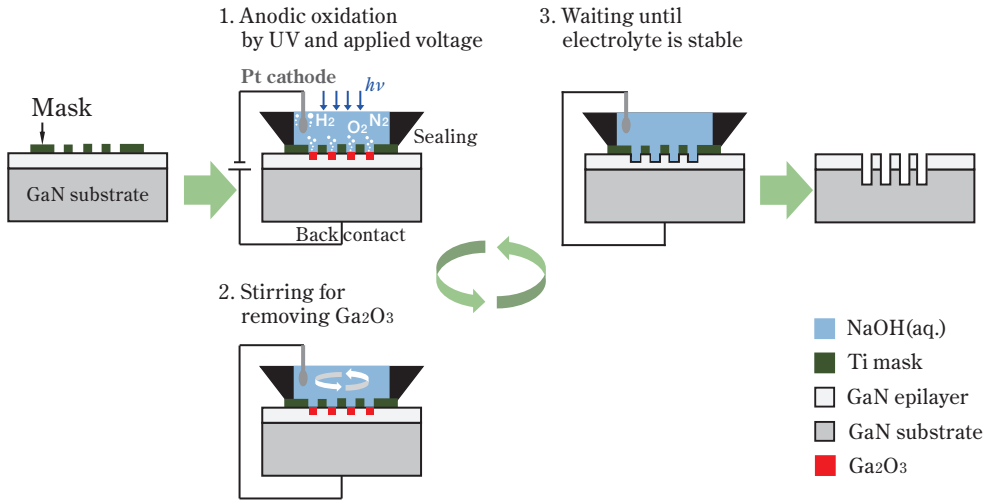

Fig. 1 Schematic representation of the conventional PEC etching of GaN[13)]

$$2H_2O(l) + 2e^- \rightarrow 2OH^- + H_2(g)\uparrow \quad (3)$$

PEC etching has succeeded in wet etching chemically stable GaN through a step of oxidizing and then dissolving the oxide instead of directly dissolving GaN. Although omitted in the above description, since the band gap of GaN is higher than the oxidation-reduction potential of water, an oxygen generation reaction occurs at the anode.

PEC etching has less etching damage than dry etching, and if a mask is appropriately selected, only the region irradiated with UV light can be selectively etched. The feature brings with it the high etching selectivity between GaN and the etching mask, and becomes available for fabricating the vertical deep trenches. Furthermore, the short lifetime of photo-generated holes realized a small amount of side etching of less than 1 μm.[13)] On the other hand, conventional PEC etching requires sealing of the electrolyte and electrical contact via an outside circuit. These simultaneous requirements presented a large constraint for experimental setups in large-scale wafer processes.

Contactless PEC etching technology

In order to eliminate the complexity of the conventional PEC etching described above, a contactless PEC etching without connection to an external circuit has been proposed.[14),15)] In contactless PEC etching, photo-generated extra electrons are consumed by the sulfate radical $SO_4^{\bullet-}$ in the electrolyte, that is, it makes it contactless. The most essential point is that the sample is only dipped into the electrolyte for etching. **Fig. 2** shows a schematic diagram of a contactless PEC etching system.

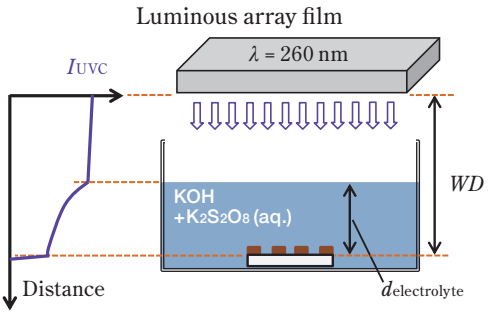

Fig. 2 Schematic illustration of the experimental setup for electrodeless PEC etching using $K_2S_2O_8$-containing solution under UVC illumination[21)]

$$GaN + \text{photocarriers}\ (3h^+ + 3e^-) + 3SO_4^{\bullet-} \rightarrow Ga^{3+} + 3SO_4^{2-} + 1/2N_2(g)\uparrow \quad (4)$$

The sulfate radical $SO_4^{\bullet-}$ is known as a strong oxidizing agent, and it is generated by peroxodisulfate ions such as potassium peroxodisulfate ($K_2S_2O_8$) solution under UV irradiation at a wavelength shorter than 310 nm (UVC). The etching conditions of the contactless PEC are summarized in **Table 1**.[14)–21)]

In previous studies, 1 kW class high-power Hg lamps or excimer lasers have been used as UV sources.

Table 1 Summary of the contactless PEC etching technologies [21]

Author	Electrolyte	UV source	Intensity (mW/cm^2)	Mask	Stirring	Rate (nm/min)
G. Parish [14]	KOH (pH=11.9-12.9) + 0.02-0.05 M $K_2S_2O_8$	HeCd 325 nm laser Hg lamp (254 nm) to illuminate only electrolyte	10 or 1000 1.1	Pt	Stirred	5-200
J. A. Bardwell [15]	0.08-0.1 M KOH + 0.08-0.1 M $K_2S_2O_8$	Hg lamp (500 W) with 254 nm mirror with 365 nm mirror	4.3 @ 254 nm 21 @ 310 nm 4.1 @ 310 nm 21.7 @ 365 nm	Pt or SiO_2	Stirred	43 @ Pt 4.8 @ SiO_2
Z. H. Hwang [16]	0.01 M KOH + 0.05 M $K_2S_2O_8$	Hg lamp (1000 W) through a water filter with mechanical chopper	9-63	Ti	Non	ND
R. T. Green [17]	0.005-0.1 M KOH + 0.1 M $K_2S_2O_8$	Hg-Xe lamp (500 W) (HeCd laser)	70 @ 365 nm (160 @ 325 nm)	Ni or Ti	With & w/o stirring	5-90
D. H. van Dorp [18]	0.02 M KOH + 0.02 M $K_2S_2O_8$	Xe lamp (500 W)	ND	Wax	With & w/o stirring	ND
J. L. Weyher [19]	0.004-0.1 M KOH + 0.01-0.1 M $K_2S_2O_8$	Xe lamp (500 W)	ND	Wax	Non	ND
S. G. Lee [20]	0.01 M KOH + 0.05 M $K_2S_2O_8$	Xe lamp (1000 W) through 345 nm long-pass filter with mechanical chopper Q-switched 355 nm laser	100 (345-364 nm) 3.0×10^5	Ti/Au	ND	30-60 5-15
F. Horikiri [21]	0.01 M KOH + 0.05 M $K_2S_2O_8$	Luminous array film (15 W) by pulsed driving	4-(8) @ 260 nm*	Ti or SiO_2	Non	5-(17) @ Ti 1 @ SiO_2

*: at the surface of electrolyte

These light sources are not preferable for mass producing large-size wafers. In addition, none of the reports regarding contactless PEC etching were discussed about a solution with an experimental geometrical setup. Thus, here, an experimental setup is discussed as well as the influence of the UVC intensity for a simple contactless PEC-etching technology for GaN.

The key point of the contactless PEC etching technology is the decomposition of $K_2S_2O_8$ in the electrolyte solution to generate $SO_4^{\bullet -}$ by UV light irradiation. On the other hand, the irradiation of UV light also acts for excitation to generate electron-hole pairs at the surface of GaN. The decomposition of $K_2S_2O_8$ requires irradiation with UV light of 310 nm or less, while excitation of GaN requires irradiation with UV light of less than 365 nm. These can be independently irradiated with separate light sources, but in order to simplify the etching apparatus, it is preferable to perform both simultaneously with one UV light source of 310 nm or less. For that purpose, it is necessary to adjust the concentration and depth of the $K_2S_2O_8$ solution so that the irradiated UV light can be used for $K_2S_2O_8$ decomposition and GaN excitation with good balance. Then we measured the transmittance of the various $K_2S_2O_8$ solutions in range of 0–0.1 M in the concentration. **Fig. 3** shows the transmittance when the depth of the $K_2S_2O_8$ solution was 1 cm. This result indicates the UVC absorption and the absorption edge shifted to a longer wavelength with the increase of the $K_2S_2O_8$ concentration. The intensities $Ix(\lambda)$ at an electrolyte depth of x (cm) are expressed as follows:

$$I_x(\lambda) = I_0 \times 10^{-\exp(-(\lambda-\lambda i)/b)\times(x/a)} \quad (5)$$

where I_0 is the intensity of the electrolyte surface, λ is the wavelength (nm), and a = 1 cm is the path-cell length. The fitting parameters λi (nm) and b (nm) are presented in **Table 2**. The result of the fitting is shown by the dotted line in **Fig. 3**. Based on the transmittance measurement, a PEC etching experiment was performed with the following configuration.

Table 2 Transmittance fitting parameters of the 0.01–0.1 M $K_2S_2O_8$ (aq.) [21]

	$K_2S_2O_8$ (aq.) (M)					
	0.01	0.02	0.04	0.06	0.08	0.10
λ_i (nm)	231.1	241.6	251.7	259.1	263.4	267.6
b (nm)	16.3	17.3	18.5	19.2	19.5	20.0

I_0 = 92.36%, a = 1 cm

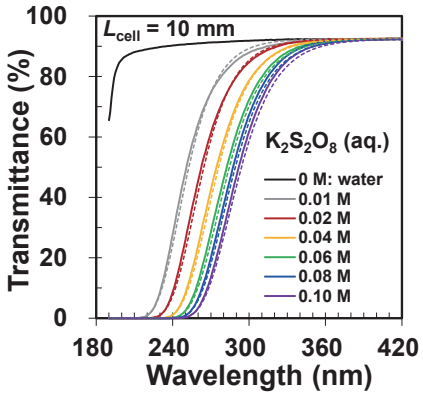

Fig. 3 Transmittance of $K_2S_2O_8$ (aq.) at various concentrations: 0 (water), 0.01, 0.02, 0.04, 0.06, 0.08, and 0.10 M. A 10 mm path-cell length was used. The solid lines correspond to experimental data. The dashed lines correspond to the fitting results, which are based on Eq. (5) with parameters from Table 2.[21]

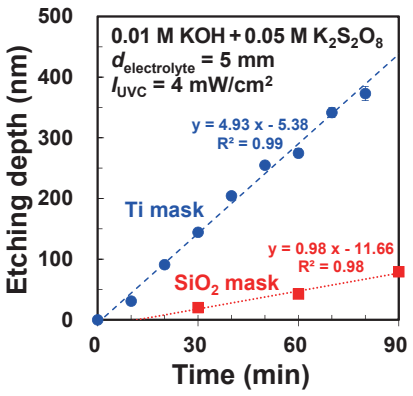

Fig. 4 Results of contactless PEC etching with a catalytic Ti mask, compared with those obtained by using an SiO_2 mask[21]

Light source: Luminous array film type deep ultraviolet plasma light source (Shikoh Tech LLC, SK-BUVC-0860)
Emission wavelength 260 nm (FWHM = 55 nm)
Electrolyte: 0.01 M KOH + 0.05 M $K_2S_2O_8$
Electrolyte depth: 5 mm
Distance from light source to electrolyte: 40 mm
The light intensity on the electrolyte surface: 4 mW/cm^2 (measured by Ushio UV illuminometer UIT-250)

The following etching experiment was performed under these conditions. The two-inch free-standing GaN substrates were used, which were produced using our void-assisted separation (VAS) method. The free-standing VAS-GaN substrate had a dislocation density of approximately 3×10^6 cm^{-2}, and the dislocations were uniformly distributed over its surface. The epitaxial layers with Schottky barrier diode (SBD) structures were grown by metal-organic vapor-phase epitaxy on n-GaN substrates. The SBDs consisted of an n-GaN layer with a nominal Si concentration of 1.0×10^{16} cm^{-3} and a thickness of 10 µm. 1 µm thick n^+ interlayer was grown between the n^- drift layer and the n-type GaN substrate. 330 nm thick SiO_2 mask was prepared by the spin-on-glass method and patterned by buffered hydrofluoric acid with a photoresist mask. In addition, in order to examine the catalytic activity effect of the mask, a sample was also prepared with 100 nm thick Ti metal film partially deposited as a mask by using electron beam lithography. **Fig. 4** shows the relationship between the etching time and the etching depth of GaN by contactless PEC etching. The etching depth of GaN is proportional to the time, and it has good controllability. The etching rate when using Ti as a mask is about 5 nm/min, which is five times larger than when using a SiO_2 mask. According to Van Dorp, Ti works as a cathode in contactless PEC, and it is reported that electrons are consumed on the Ti surface to generate hydrogen.[18] The difference of the etching rates between the SiO_2 and the Ti mask might be caused by this phenomenon. That is, in an insulating SiO_2 mask, photo-generated electrons are not consumed on the SiO_2 surface, and the electrons must be

consumed at the surface of the side-wall and/or the back surface of the sample as a cathode. These phenomena suggest that in the contactless PEC etching of GaN, it is important how to design and form the cathode on the sample.

Fig. 5 shows an atomic force microscopy (AFM) image of the sample surface obtained by etching the GaN crystal by 98 nm using contactless PEC technique. The surface roughness of the sample was 2.26 nm in RMS, and a very flat etched surface was obtained. The etched surface has very small bumps, whose number corresponds to the dislocation density of the substrate of 10^6 cm^{-2}. Thus, near a dislocation, where the carrier lifetime is short, the anodic oxidation reaction was suppressed by the [h^+] supply limit. The bump can be eliminated through the application of high-intensity UV irradiation. We also confirmed that the bumps can be removed by post treatment by 25 wt% tetramethylammonium hydroxide (TMAH) aqueous solution at 85 °C for 30–60 minutes.[22)]

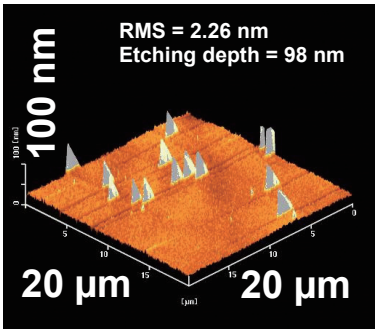

Fig. 5 AFM images of electrodeless PEC-etched GaN surface under UVC irradiation conditions for 98 nm etching depth[21)]

PEC etching with acidic electrolyte

For the PEC etching of GaN reported so far, an alkaline solution such as an aqueous solution of KOH or NaOH as an electrolyte is used, regardless of the presence or absence of an external circuits. However, in particular, in contactless PEC etching, generated SO_4^{2-} by the decomposition of $K_2S_2O_8$ causes pH to decrease. Therefore, when a basic electrolyte is used, the pH changes from basic to acidic with UV light irradiation. There is a disadvantage that the etching rate is not stable depending on the conditions. Furthermore, in the general device fabrication process, photoresist is used as a mask of photolithography technique, but photoresist is resistant to acid but weak to basic, and peels off in liquid. For this reason, it has been complicated to form a mask pattern by performing photolithography using a photoresist after depositing a metal film such as SiO_2 or Ti on an epiwafer.

Instead of basic KOH, we chose acid-based H_3PO_4 as the electrolyte and worked on acid-based PEC etching.[23)] The sample used for the experiment was obtained by homoepitaxially growing n-type GaN by MOCVD on an n-type GaN substrate manufactured on our production line. The carrier concentration, thickness, and dislocation density of the epilayer were 5×10^{16} cm^{-3}, 3 μm, and 3×10^6 cm^{-2}, respectively. A positive photoresist (Megaposit™SPR6810) was applied to the surface of the epilayer with a spin coater at 950 nm, and a 10 μm-wide stripe pattern was formed by photolithography, followed by post-baking at 110 °C × 10 min. The electrolyte used for the contactless PEC etching was 0.01 M H_3PO_4 + 0.05 M $K_2S_2O_8$. For comparison, an experiment using an electrolytic solution of 0.01 M KOH + 0.05 M $K_2S_2O_8$ was also performed. Other configurations of the etching apparatus are the same as those described in the previous section.

Fig. 6 shows how the pH of the electrolyte changes over time when the H_3PO_4-based electrolyte and the KOH-based electrolyte are irradiated with UV light.[24)] **Fig. 6** indicates that the H_3PO_4-based electrolytic solution has a small change in pH over time. **Fig. 7** shows the relationship between the etching time and the

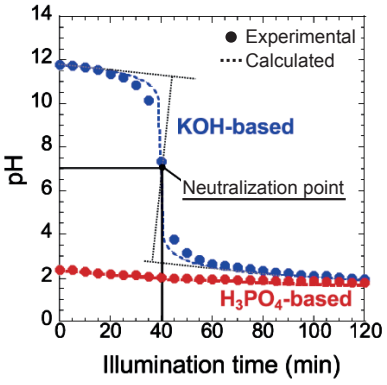

Fig. 6 Correlation between pH value of solution and illumination time of UVC light
Dashed lines indicate theoretical curves obtained with the H^+ ion production rate of 1.54×10^{-4} M/min[23)]

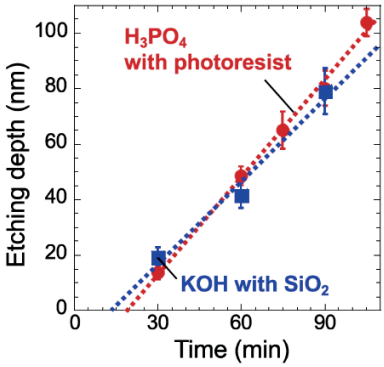

Fig. 7 Etching depth plotted as a function of etching time using H_3PO_4-based solution and KOH-based solution [23)]

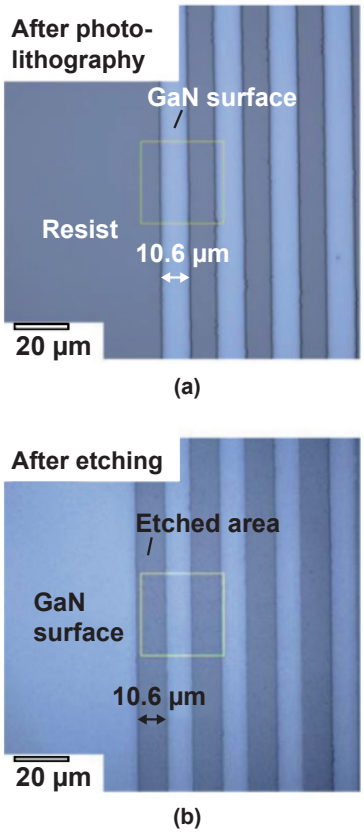

Fig. 8 Top-view images of sample with patterned-photoresist film (a) before and (b) after the etching [23)]

etching depth when etching was performed using both electrolytes. Either of the electrolyte solutions provided almost the same etching rate, or the linearity of the graph, that is, the controllability of the etching depth was good. **Fig. 8** shows the surface scanning electron microscopy (SEM) images before and after the etching of the sample etched using the H_3PO_4-based electrolyte. **Fig. 8** (a) shows a state in which a resist mask is attached to the GaN surface before etching, and **Fig. 8** (b) shows a GaN surface after etching and removing the resist mask. As a result, it was confirmed that the same good selectivity as that of a SiO_2 mask or the like was obtained even by etching using a photoresist as a mask. From the above examination, it was confirmed that an acid-based electrolytic solution could be used in contactless PEC etching, and the application range of PEC etching was significantly expanded. For example, a case in which contactless acid-based PEC etching is applied to the formation of recesses in HEMTs has been reported.[25)]

Device process application of PEC etching technology

In parallel with the development of the contactless PEC etching technology described above, we made demonstrations of various pattern processing using PEC etching with a contact in order to obtain an outlook on the extent to which PEC etching can be applied to GaN device processes. And at the same time, we appealed the effectiveness of PEC etching for our customers, device manufacturers.[12),13),22)] In addition, PEC etching was applied to the mesa formation process in the actual manufacturing process of the PN diode, and the characteristics were compared with those of a diode manufactured by conventional dry etching.[25)] These results are introduced in this chapter.

Fig. 9 shows SEM images of a sample obtained by performing PEC etching with a circular Ti mask attached to an epi having a PN diode structure. A vertical cylindrical shaped pattern is obtained clearly, and there is almost no side etching. This is due to the short lifetime of holes generated in GaN, and indicates that only the portion irradiated with UV light can be selectively etched. **Fig. 10** is an SEM image of a sample obtained by etching a 7.7 μm in depth with a circular opening mask pattern of ϕ1, 5, 10, and 20 μm attached to the epi of the SBD structure. **Fig. 11** shows cross-sectional SEM images of samples by using a stripe mask pattern having a width of 1.4, 2.8, and 5.6 μm attached to the epiwafers of the SBD structure. Etching has been completed sharply until the groove depth reaches 33 μm, indicating that PEC etching can be widely applied not only to the formation of recessed structures and mesa structures, but also to

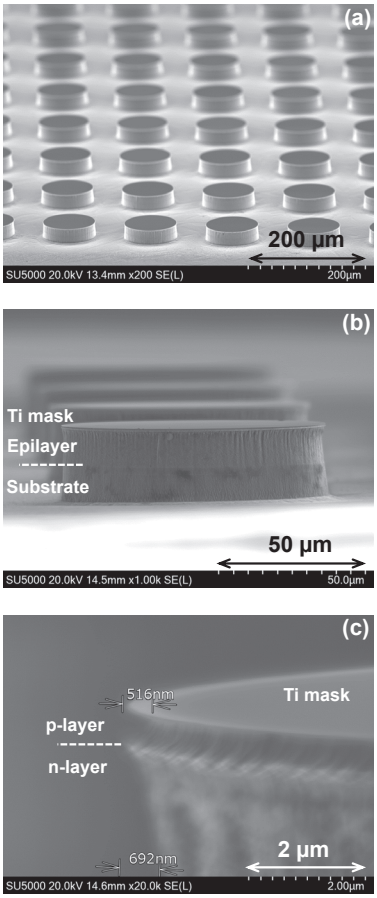

Fig. 9 SEM images of PEC-etched cylinder patterns: (a) Overhead view, (b) side view, and (c) near Ti mask and pn-junction[13)]

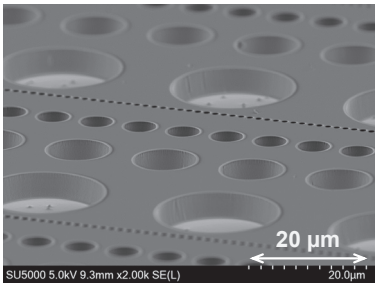

Fig. 10 SEM image of PEC-etched GaN SBD with an etching depth of approximately 7.7 μm. The diameters of the circular cavities were designed to be 1, 5, 10, and 20 μm.[13)]

element isolation and groove formation of super junction structures. **Fig. 12** shows SCIOCS's logo pattern formed on GaN using PEC etching technology as a demonstration. Etching of such a fine structure is also possible.

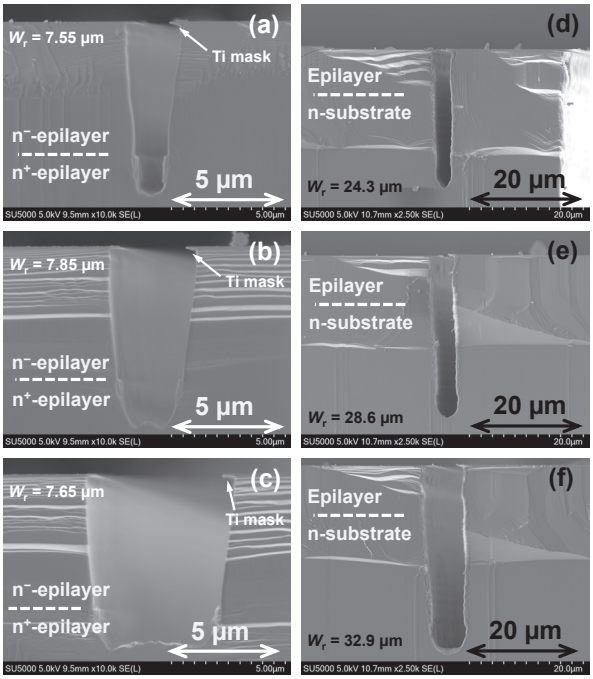

Fig. 11 Typical cross-sectional SEM images of the PEC etched trench patterns. The design PEC etching depth and Ti mask width were (a) Wr=7.7 μm and 1.4 μm, (b) Wr=7.7 μm and 2.8 μm, (c) Wr=7.7 μm and 5.6 μm, (d) Wr=33 μm and 1.4 μm, (e) Wr=33 μm and 2.8 μm, (f) Wr=33 μm and 5.6 μm, respectively.[13)]

Fig. 12 PEC etched logo pattern of our company "SCIOCS"

The trial production of PN diodes is also evaluated. **Fig. 13** is a schematic cross section showing the structure of a PN diode. PEC etching was applied to the mesa processing of this diode. **Fig. 14** shows an SEM image of a mesa shape formed by PEC etching. For comparison, a mesa shape formed by ICP dry etching is also shown. PEC etching provides a smoother surface, and we confirmed the low etching damage by photoluminescence measurements. Comparing the current-voltage (I-V) properties of the fabricated diodes, there is almost no difference in the forward

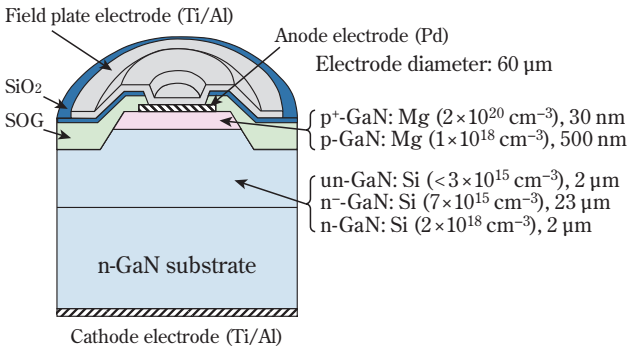

Fig. 13 Schematic cross-sectional structure of the GaN PN junction diode

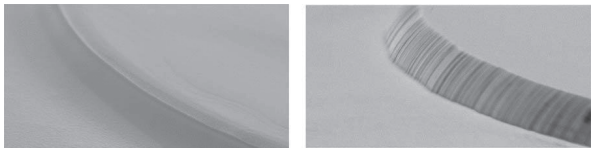

Fig. 14 SEM images of the mesa areas by PEC etching (left) and dry etching (right) [26]

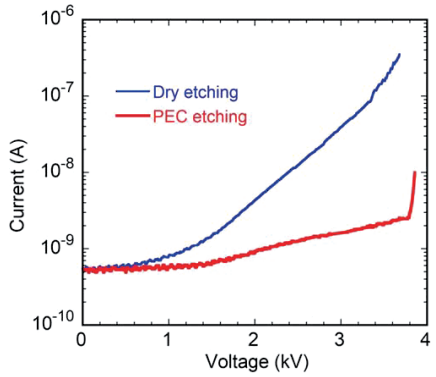

Fig. 15 Reverse I–V characteristics of the diodes fabricated by PEC etching and dry etching [26]

bias direction, but there is a remarkable difference in the reverse direction. **Fig. 15** shows a graph of the reverse I-V curves of PN diodes fabricated by PEC etching and dry etching. It clearly shows that the diode manufactured by PEC etching has a smaller leak current and a higher breakdown voltage. **Fig. 16** shows the variation of the breakdown voltage measured in each of the six diodes. Diodes fabricated by PEC etching have clearly higher breakdown voltage and less variation. This indicates that etching damage at the

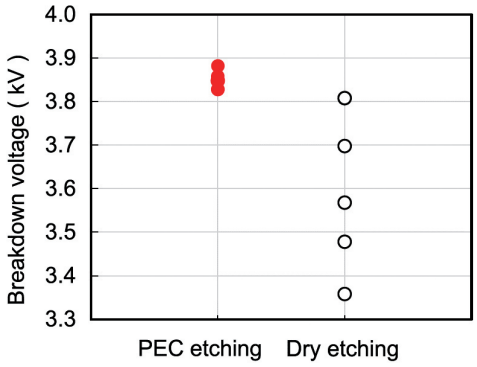

Fig. 16 Variations in the breakdown voltage of the diodes fabricated by PEC etching and dry etching [26]

mesa edge gives rise to a leakage path of current, and that PEC etching with a small amount thereof greatly contributes to improving device reliability.

Toward popularizing PEC etching technology

Although the contactless PEC etching technique of GaN is already known, there are few patent applications related to it, and it is still possible to obtain a basic patent right. If basic device patents are held down by specific device manufacturers, it will be difficult to popularize PEC etching, and it will not be possible to contribute to expanding the GaN device market. Therefore, we are vigorously applying for patents on possible basic PEC etching technology and equipment so that device manufacturers can freely use PEC etching.[27]

PEC etching is a technology for maximizing the device performance on the manufacturing process combined with our products, GaN substrates and GaN epiwafers. In other words, PEC etching technology itself does not contribute to the production of our products, but is only useful in our customer's process. It is important to popularize this convenient PEC etching technology to the GaN device community through international conferences and academic papers. Furthermore, we are developing a commercially available apparatus for contactless PEC etching. It is also important to provide it to the market at an affordable price. Therefore, we provided PEC etching technical guidance to Sanmei Co., Ltd., which manufactures and sells mask aligners and nanoimprint equipment, and licenses the above-mentioned patents to develop a PEC etching apparatus. **Fig. 17** is a poster of the PEC apparatus

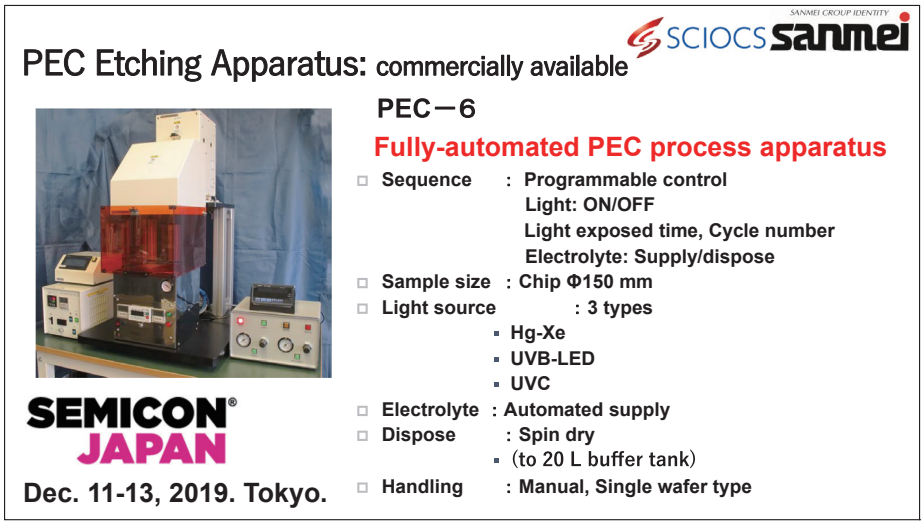

Fig. 17 Poster of the PEC etching apparatus presented in SEMICON JAPAN 2019 by SANMEI Co., Ltd.

under development, which was displayed at the booth of Sanmei Co., Ltd. at SEMICON Japan in 2019. The equipment is currently being prepared for launch in mid-2020.

Conclusion

Compared to the same wide band gap material of SiC, GaN has a delayed start in research and development, so the development of process technology has been delayed and has not spread. The contactless PEC etching technology provides minimal damage to the GaN process and brings out higher device performance. We expect that the spread of this technology will greatly expand the GaN device market.

Acknowledgement

A part of this study was supported by the Ministry of the Environment, "Technology Innovation Project for Creating the Future Society and Lifestyle." We also thank Dr. Taketomo Sato, Associate Professor of Research Center for Integrated Quantum Electronics, Hokkaido University and Prof. Tomoyoshi Mishima of Ion Beam Engineering Institute, Hosei University.

Reference

1) S. Fujita, Jpn. J. Appl. Phys., 54, 030101 (2015).
2) F. Yamaki and S. Sano, Proc. CS ManTech, 004-5 (2018).
3) H. Amano *et al.*, J. Phys. D: Appl. Phys., 51, 163001 (2018).
4) W. Saito *et al.*, Solid-State Electron., 48, 1555 (2004).
5) D. Zhuang, and J. H. Edgar, Mater. Sci. Eng., R 48, 1 (2005).
6) M. S. Minsky *et al.*, Appl. Phys. Lett., 68, 1531 (1996).
7) C. Youtsey *et al.*, Appl. Phys. Lett., 71, 2151 (1997).
8) H. Lu *et al.*, J. Electrochem. Soc., 144, L8 (1997).
9) H. Cho *et al.*, J. Electron. Mater., 28, 290 (1999).
10) I. M. Huygens *et al.*, J. Electrochem. Soc., 147, 1797 (2000).
11) J. Skriniarova *et al.*, J. Vac. Sci. Technol., B19, 1721 (2001).
12) F. Horikiri *et al.*, Jpn. J. Appl. Phys., 57, 086502 (2018).
13) F. Horikiri *et al.*, Appl. Phys. Express, 11, 091001-1 (2018).
14) G. Parish *et al.*, Proc. SPIE, 4592 (2001).
15) J. A. Bardwell *et al.*, J. Appl. Phys., 89, 4142 (2001).
16) Z. H. Hwang *et al.*, Appl. Phys. Lett., 84, 3759 (2004).
17) R. T. Green *et al.*, J. Electron. Mater., 36, 397 (2007).
18) D. H. van Dorp *et al.*, J. Electrochem. Soc., 156, D371 (2009).
19) J. L. Weyher *et al.*, J. Cryst. Growth, 312, 2607 (2010).
20) S. G. Lee *et al.*, Appl. Phys. Express, 10, 011001 (2017).
21) F. Horikiri *et al.*, Appl. Phys. Express, 12, 031003 (2019).
22) F. Horikiri *et al.*, IEEE Trans. Semicond. Manuf., 32, 489 (2019).

23) M. Toguchi *et al*., Appl. Phys. Express, 12, 066504 (2019).
24) F. Horikiri *et al*., Appl. Phys. Express, 13, 046501 (2020).
25) K. Miwa *et al*., Appl. Phys. Express, 13, 026508 (2020).
26) N. Asai *et al*., Jpn. J. Appl. Phys., 58, SCCD05 (2019).
27) e.g., SCIOCS Co., Ltd., Sumitomo Chemical Co., Ltd., JP 6625260 B1 (2019), JP 6668545 B1 (2020), etc.

PROFILE

Fumimasa Horikiri
SCIOCS COMPANY LIMITED
Business Development Department
Ph. D.

Masatomo Shibata
SCIOCS COMPANY LIMITED
Business Development Department

Noboru Fukuhara
SCIOCS COMPANY LIMITED
Business Development Department